Enhanced-Resolution SSM/I and AMSR-E Daily Polar Brightness Temperatures, Version 1

USER GUIDE

How to Cite These Data

As a condition of using these data, you must include a citation:

Long, D. G. and J. Stroeve. 2011. *Enhanced-Resolution SSM/I and AMSR-E Daily Polar Brightness Temperatures, Version 1*. [Indicate subset used]. Boulder, Colorado USA. NASA National Snow and Ice Data Center Distributed Active Archive Center. https://doi.org/10.5067/MES22DNFS3O8. [Date Accessed].

FOR QUESTIONS ABOUT THESE DATA, CONTACT NSIDC@NSIDC.ORG

FOR CURRENT INFORMATION, VISIT https://nsidc.org/data/NSIDC-0464

National Snow and Ice Data Center

TABLE OF CONTENTS

1 DETAILED DATA DESCRIPTION

This data set contains enhanced-resolution brightness temperatures produced using the Scatterometer Image Reconstruction (SIR) algorithm developed by the Microwave Earth Remote Sensing (MERS) group at Brigham Young University (BYU). Enhanced-resolution brightness temperature images for the Arctic and Antarctic were generated using antenna temperature data from the Special Sensor Microwave/Imager (SSM/I) and the Advanced Microwave Scanning Radiometer - Earth Observing System (AMSR-E) instrument. SSM/I images are available for 1995 through 2008, and AMSR-E images are available for 2002 through 2011. All available measurements for a single day are averaged into twice-daily gridded files for three different equal-area spatial coverages: Northern Hemisphere, Southern Hemisphere, and full global. The spatial resolution is 12.5 km for SSM/I channels 19 and 22 GHz, 7.5 km for 37 GHz, and 2.5 km for the 85 GHz channel. For AMSR-E, the resolution is 12.5 km for the 6, 10, 18, and 23 GHz channels; 7.5 km for the 36 GHz channel; and 2.5 km for the 89 GHz channel. Software for reading the SIR-formatted SSM/I and AMSR-E data is also available. As scatterometer and radiometer data complement each other, these enhanced-resolution radiometer data, together with SIR format scatterometer data available from BYU, will facilitate polar research that combines information from both radiometers and scatterometers. Data are stored as scaled 2-byte integers in binary arrays with a 512-byte header.

1.1 Format

Data are provided in zipped binary files, and are stored as scaled 2-byte integers representing brightness temperature values ranging from 100 K to 427.67 K. A factor of 200 is applied to the brightness temperature value minus 100 prior to converting the value to an integer. Conversion from integer value K to brightness temperature is given in the formula Tb=100+K/200. For example, a stored integer value of 2358 represents a brightness temperature value of 111.79 K. A value of 0 represents missing data. Note that these scale factors and the projection parameters are contained in the file header so they can be used by the available file readers.

1.2 File and Directory Structure

Data are available on the HTTPs site in the https://daacdata.apps.nsidc.org/pub/DATASETS/nsidc0464_enhanced_ssmi_amsre_tbs/ directory. The directory is divided into two main folders: `amsre and ssmi`. The two main folders are further broken down by yearly folders. The yearly folders for both the data and browse imagery are then divided into three subfolders: `global, north,` and `south`.

1.3 File Naming Convention

Table 1 explains the file naming convention used for this product with an example.

Examples:

```
AMSRE_hirz_2008165n_EaM37h_v01.sir.gz
SSMIF13_hirz_2008165n_EaN22v_v01.gif
IIII(I)(ppp)_hirz_yyyydoyt_EaXCCc_vVV.sir.gz
```

Table 1. File Naming Convention Values

Variable	Description
IIII(I)	Instrument (SSMI, AMSRE)
(ppp)	SSM/I platform (F13)
hirz	Indicates data are high-resolution
YYYY	4-digit year
doy	3-digit day of year
t	Time of day (m: morning, a: afternoon, e: evening, n: night)
Ea	EASE-Grid projection
X	EASE-Grid projection region (N: North, S: South, M: Global)
CC	Channel frequency (06, 10, 18, 19, 22, 23, 36, 37, 85, 89)
c	Channel polarization (v: vertical, h: horizontal)
vVV	Data version number (for example, v01)
.sir	Indicates file format is Scatterometer Image Reconstruction (SIR)
.gz	Indicates file has been compressed using Gzip
.gif	Indicates this is a GIF image file

1.4 File Size

All brightness temperature data files are compressed using Gzip, as indicated by the gz file extension. Note that browse image files are not zipped, and range in size from approximately 5 KB to 7 MB.

Whether zipped or unzipped, SSM/I and AMSR-E data file sizes vary depending on the region and/or frequency, as shown in Tables 2 and 3, respectively. File sizes are approximate.

Table 2. SSM/I File Sizes

Region	SSM/I Channels (GHz)	Zipped Size (MB)	Unzipped Size (MB)
North	85.5	21	63
North	19.3 22.2 37.0	0.2 0.2 6	4 4 16
South	85.5	18	63
South	19.3 22.2 37.0	0.2 0.2 4.5	4 4 16
Global	85.5	0.08	1.5
Global	19.3 22.2 37.0	0.08 0.08 0.5	1.5 1.5 1.5

Table 3. AMSR-E File Sizes

Region	AMSR-E Channels (GHz)	Zipped Size (MB)	Unzipped Size (MB)
North	89.0	1	4
North	6.9 10.7 18.7 23 36.5	1 1 1 1 1	4 4 4 4 4
South	89.0	1	4
South	6.9 10.7 18.7 23 36.5	1 1 1 1 1	4 4 4 4 4
Global	89.0	0.5	1.5
Global	6.9 10.7 18.7 23 36.5	0.5 0.5 0.5 0.5 0.5	1.5 1.5 1.5 1.5 1.5

1.5 Volume

Unzipped, the total volume of this data set is approximately 4.3 TB. When zipped, it is 1 TB.

1.6 Spatial Coverage

These data files are provided in three different equal-area, spatial coverages: Northern Hemisphere azimuthal, Southern Hemisphere azimuthal, and global cylindrical. Please see the Grid Extent Table on the EASE-Grid web page for specific latitude and longitude values. Figure 1 shows a map of the three different coverages.

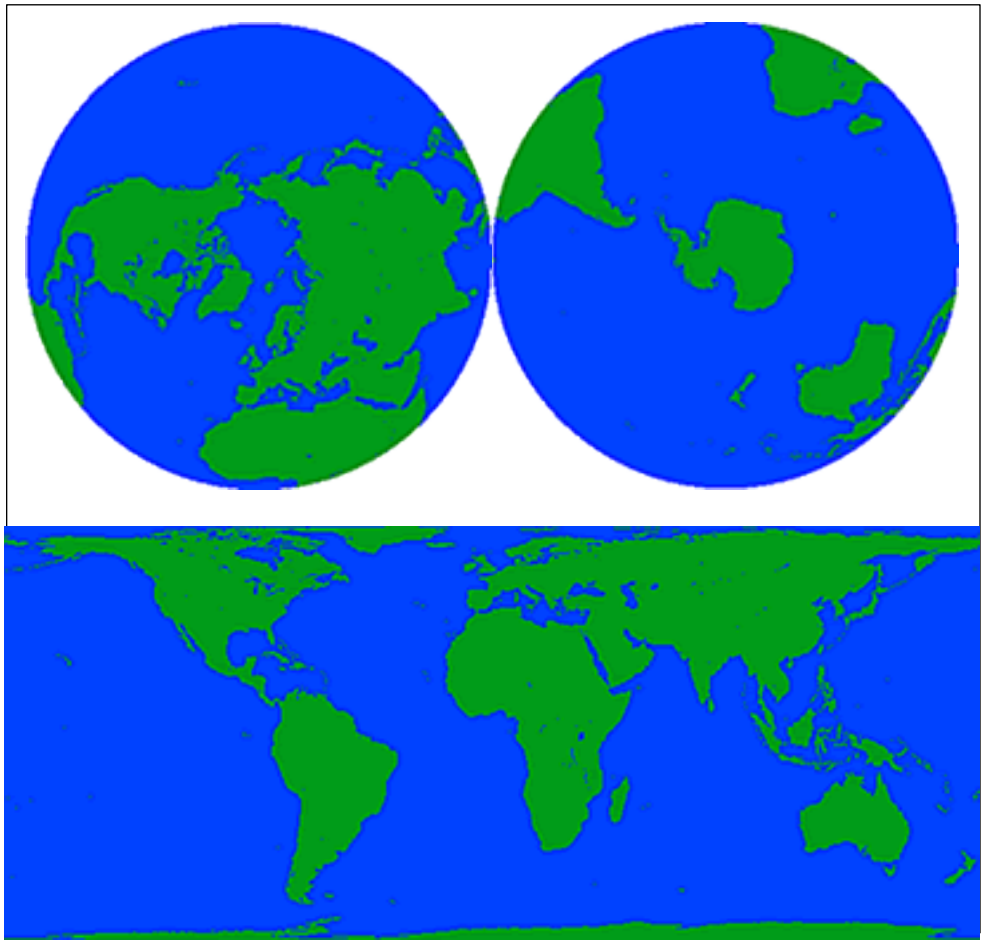

Figure 1. Top two images: coverage of Northern and Southern Hemispheres (based on Lambert's equal-area, azimuthal projection). Bottom image: global coverage (based on cylindrical, equal-area projection).

1.6.1 Spatial Resolution

The low-frequency channel resolution of this data set is similar to European Space Agency (ESA) Earth Remote Sensing (ERS) scatterometer images, while the high-frequency channel resolution is similar to that of NASA Scatterometer (NSCAT) and Seawinds scatterometer images. The spatial resolution is 12.5 km for SSM/I channels 19.3 and 22.2 GHz (in 1441x1441 arrays), 7.5 km for 37.0 GHz (in 2881x2881 arrays), and 2.5 km for the 85.5 GHz channel (in 5761x5761 arrays). The

resolution for AMSR-E 6.9, 10.7, 18.7, 23.8, and 36.5 GHz channels is 12.5 km; the 36.5 GHz is 7.5 km; and the 89.0 GHz channel is 2.5 km.

1.6.2 Projection and Grid Description

The SSM/I and AMSR-E EASE-Grids are a set of three equal-area projections: two azimuthal equal-area projections, one for the Northern and one for the Southern Hemisphere; and a global cylindrical equal-area projection. Please see the EASE-Grid web page for more information on the EASE-Grid.

1.7 Temporal Coverage

Temporal coverage for the SSM/I data spans 1995 through 2008, and 2002 through 2011 for AMSR-E.

1.7.1 Temporal Resolution

Twice-daily enhanced-resolution brightness temperature images were generated for the Arctic and Antarctic using SSM/I and AMSR-E data

1.8 Parameter or Variable

1.8.1 Parameter Description

Theoretically, brightness temperature is the effective temperature of a blackbody radiating the same amount of energy per unit area at the same wavelengths as the observed body. Empirically, brightness temperature is the apparent radiant temperature of a non-blackbody determined by measurement with an optical pyrometer or radiometer. The brightness temperature (Tb) at a given wavelength (Λ) is the product of the physical temperature (Tp) and the emissivity (Σ) at the given wavelength of the surface viewed by the radiometer. Refer to Equation 1.

$$Tb(\Lambda) = \Sigma(\Lambda)Tp \qquad \textbf{(Equation 1)}$$

Equation 1 is the Rayleigh-Jean approximation of Plank's law for the passive microwave region of the electromagnetic spectrum. It is an approximation and does not take into account effects of the atmosphere on the microwave radiation.

Table 4 compares the channels for each instrument at which the brightness temperatures for this data set are calculated. As indicated in the table, with the exception of 22.2 GHz, each frequency is both vertically and horizontally polarized.

Table 4. Comparable Channels of SSM/I and AMSR-E Instruments

SSM/I	AMSR-E
N/A	6.9V, 6.9H
N/A	10.7V, 10.7H
19.3V, 19.3H	18.7V, 18.7H
22.2V	23.8V, 23.8H
37.0V, 37.0H	36.5V, 36.5H
85.5V, 85.5H	89.0V, 89.0H

1.8.2 Parameter Range

Data are stored as scaled 2-byte integers representing brightness temperature values, ranging from 100 K to 427.67 K. A factor of 200 is applied to the brightness temperature value minus 100 prior to converting the value to an integer. Conversion from integer value K to brightness temperature (Tb) is given in the formula Tb=100+K/200. For example, a stored integer value of 2358 represents a brightness temperature value of 111.79 K. A value of 0 represents missing data. Note that these scale factors and the projection parameters are contained in the file header so they can be used by the available file readers.

1.8.3 Unit of Measurement

Brightness temperatures are measured in kelvins (K), and are precise to .01 K.

1.9 Sample Browse Images

Figure 2 displays sample browse images acquired from the 89 GHz SSM/I channel (top) and the AMSR-E 85 GHz channel (bottom).

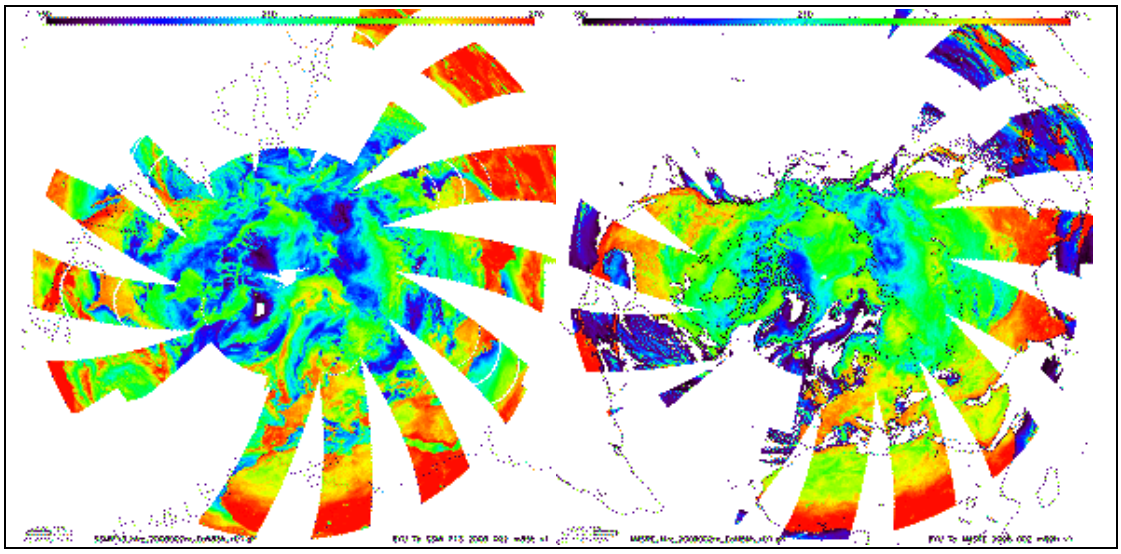

Figure 2. Sample Browse Images for the Northern Hemisphere Morning H-pol Brightness Temperatures

2 SOFTWARE AND TOOLS

The following IDL tools are available via FTP in the directory named `idl`.

These IDL programs were written by BYU-MERS and redistributed at NSIDC for user convenience. Please read the `readme` file for instructions on using them. Other IDL and MATLAB programs are available from BYU-MERS. The IDL code may be copied and modified as long as original or modified code is not redistributed for profit, and acknowledgement is made that the original code was obtained courtesy of David G. Long at the Microwave Earth Remote Sensing Laboratory at Brigham Young University.

2.1 Interactive Data Language (IDL) Programs

loadsir.pro: Simple program to read and display SIR files. Use the following command at the IDL prompt to display a SIR file in a 512 by 512 window:

```
loadsir,'filename.sir.mask',array,info
sirimage=congrid(array,512,512)
tvscl,sirimage
```

xsir.pro: A more robust program to read and display SIR files. This program calls a number of IDL subroutines contained in other files, including `pixtolatlon.pro, ilambert1.pro, ipolster.pro,` and `ieasegrid.pro`. These routines convert pixel location to lat/lon (`pixtolatlon.pro`) or lat/lon to pixel location (`latlon2pix.pro`) based on the info array containing the file header information.

2.2 Fortran Programs

Code is provided to read SIR files using Fortran 77 and Fortran 90. Utilities are also provided to convert SIR images to other file types (byte).

2.3 Quality Assessment

Enhanced SSM/I brightness temperatures were produced without calibration changes from the Remote Sensing Systems (RSS) Version 6 (V6) SSM/I swath product for DMSP-F13. Enhanced AMSR-E brightness temperatures were produced, also without adjustments, from the RSS V4 AMSR-E swath product. For details regarding calibration and validation of these source products, please visit RSS.

3 DATA ACQUISITION AND PROCESSING

3.1 Theory of Measurements

Microwave radiometers such as SSM/I and AMSR-E have wide application in atmospheric remote sensing over the ocean and provide essential inputs to numerical weather-prediction models. SSM/I and AMSR-E data have also been used for land and ice studies, including snow-cover classification, measurements of soil and plant moisture content, atmospheric moisture over land, land surface temperature, and mapping polar ice. Unfortunately, the relatively low resolution of SSM/I and AMSR-E is a limiting factor in their application for other land and ice studies. The intrinsic horizontal resolution of both instruments is determined by the antenna-beam pattern and, depending on the channel, its resolution varies from approximately 70 to 15 km. To ameliorate this limitation, resolution-enhancement algorithms can be applied to the data. Resolution enhancement is, in effect, equivalent to antenna-pattern deconvolution. Two resolution-enhancement algorithms developed for microwave data are the Backus Gilbert Inversion (BGI) method, which has been applied to SSM/I data for both resolution enhancement and optimal interpolation, and the scatterometer image reconstruction (SIR) algorithm. The SIR algorithm was originally developed for SEASAT-A scatterometer data, but since scatterometer and radiometer data compliment each other, it has been adapted for use with SSM/I and AMSR-E data. The SIR algorithm requires less computation than the BGI method. See Long and Daum (1998) for a comparison of these two algorithms in generating enhanced resolution brightness images from SSM/I and AMSR-E data over land areas.

Note that both the BGI and SIR resolution enhancement algorithms generate images from the radiometer measurements. While they effectively deconvolve the antenna pattern, the algorithms do not enhance previously produced images as do image-processing algorithms; rather, they are

reconstruction algorithms, which attempt to reconstruct the underlying brightness distribution (Tb) on a high-resolution grid from lower resolution measurements. And while the grid can be made arbitrarily fine, the resolution enhancement capabilities of both the BGI and SIR algorithms are dependent on the sampling pattern and the overlap in the response functions of the measurements. In general, the higher the sampling density (leading to more overlap in the measurements), the better the resolution enhancement. Note that an overly fine grid increases the computational requirements without improving the effective resolution of the output image. Like all resolution-enhancement techniques, both algorithms provide improved resolution at the expense of an increased noise level in the images. (Long and Daum 1998)

3.2 Data Acquisition Methods

The input brightness temperatures used for this data set were acquired from the SSM/I instrument mounted on the DMSP-F13 satellite, and from the AMSR-E instrument on the NASA Aqua satellite.

Input brightness temperatures from the SSM/I and AMSR-E instruments were acquired from Remote Sensing Systems (RSS), Santa Rosa, California (Wentz 1993). The input data were then processed and enhanced by the BYU MERS Laboratory.

3.3 Derivation Techniques and Algorithms

The following has been adapted from Long and Daum (1998), pp. 408-410:

The SIR algorithm, originally designed to produce multivariate scatterometer images, has been adapted for radiometer measurements. It produces radiometric images by using an iterative procedure from an initial brightness estimate. The procedure is nonlinear and depends on the antenna pattern dimension, shape, and measurement overlap to obtain resolution enhancement. The SIR algorithm is a variation of the multiplicative algebraic-reconstruction technique (MART), a maximum entropy reconstruction method. The detailed derivation for scatterometer data is found in Long et al. (1993) with further elaboration in Early and Long (2001), and the radiometer version of the algorithm is provided in its entirety in Long and Daum 1998.

Ignoring the effects of the atmosphere, an SSM/I measurement can be modeled as a product of the surface brightness and the antenna pattern. The *i*th measurement `Ta(i)`, in K, is obtained by integrating the product of surface brightness response `Tb(x,y)`, in K, and the antenna at the surface `Gi(x,y)`:

Where:

$$T_a(i) = \overline{G}_i^{-1} \iint G_i(x, y) T_b(x, y)\, dx\, dy$$ **(Equation 2)**

Where:

$$\overline{G}_i = \iint G_i(x, y)\, dx\, dy$$ **(Equation 3)**

where integrals are over the surface area corresponding to the non-negligible gain of the antenna. The dependence of G on i arises from the boresight pointing of the antenna, which changes as the antenna scans the surface. Note that the antenna pattern acts as a non-ideal, low-pass filter of the surface brightness.

SIR provides a maximum-entropy estimate of the brightness temperature for each element of a rectilinear grid of pixels. Assuming that the brightness temperature is constant within each pixel, Equation 2 can be written as:

$$T_a(i) = \frac{1}{\overline{G}_i} \sum_{x=L_i}^{R_i} \sum_{y=B_i}^{T_i} T_b(x, y) G_i(x, y)$$ **(Equation 4)**

Where:

$$\overline{G}_i = \sum_{x=L_i}^{R_i} \sum_{y=B_i}^{T_i} G_i(x, y)$$ **(Equation 5)**

and L_i, R_i, B_i, and T_i define a bounding rectangle for the *i*th measurement. In implementing the SIR algorithm, an initial guess for the T_b image is first made, typically the average expected brightness temperature. A predicted value, or forward projection, of each measurement is calculated from a current estimate of T_b and is compared to the measurement. A scale factor is then computed as the ratio of the measurement to the forward projection. An update term is computed for each pixel in the measurement cell by multiplying by the scale factor. Between iterations, each pixel in the image is updated by averaging the update terms for the pixel. As the process iterates, the scale factors approach unity and all of the forward projections match the measurements. When noise is present in the measurements, however, the scale factors may not always converge to unity. In such a case, the algorithm attempts to balance the various scale factors for each measurement and pixel using

maximum entropy. In SIR, the scale factors calculated for each forward projection are damped by taking the square root. In addition, the update terms are computed in a manner that limits the amount of change for a single update (refer to Equation 9). These steps tend to reduce the sensitivity of the update terms to noise.

Let `Tb(x,y)` be denoted by `Pj` and `Gi(x,y)` by `Hij` where `j` is the row-scanned pixel number and `i` is the measurement number. Then for the kth iteration, and for the `i`th measurement in the data set `zi` and its corresponding weighting function, `hij`, the forward projection,

$$f_i^k$$

is calculated as:

$$f_i^k = \frac{1}{q_i} \sum_{n=1}^{M} h_{in} p_n^k$$

$$q_i = \sum_{n=1}^{M} h_{in}$$

(Equations 6 and 7)

where `M` is the number of pixels in the image. The scale factor,

$$d_i^k$$

is then computed as:

$$d_i^k = \left[\frac{T_a(i)}{f_i^k} \right]^{1/2}.$$

(Equation 8)

The non-linear update term,

$$u_{ij}^k$$

is then computed according to:

$$u_{ij}^k = \begin{cases} \left[\frac{1}{2f_i^k}\left(1-\frac{1}{d_i^k}\right)+\frac{1}{p_j^k d_i^k}\right]^{-1}, & d_i^k \geq 1 \\ \left[\frac{1}{2}f_i^k(1-d_i^k)+p_j^k d_i^k\right], & d_i^k < 1. \end{cases}$$

(Equation 9)

After the entire data set has been processed, each pixel estimate,

$$p_j^k$$

is updated by computing a weighted average of the update terms, as shown in Equation 10, where N_m is the number of measurements:

$$p_j^{k+1} = \frac{1}{g_j}\sum_{i=1}^{N_m} h_{ij}u_{ij}^k$$

$$g_j = \sum_{i=1}^{N_m} h_{ij}.$$

(Equation 10)

This set of equations is iterated over k for N iterations until the scale factors approach unity. Because of the damping employed in the update terms, the algorithm always converges and the iteration may be continued even for very large k values. As shown in the next section, however, the accuracy of the algorithm at first increases with the iteration number, but then may decrease as the iteration continues. This is a common problem with algebraic reconstruction algorithms and is the result of excessive noise amplification. Fortunately, the algorithm's performance is not particularly sensitive to the exact number of iterations used and a range of values will produce good results. This range depends on the antenna pattern size and sampling density. In Long and Daum (1998), simulation was used to determine the optimum number of iterations to use for each channel. With SSM/I data, for example, convergence is typically obtained within 15 iterations.

3.3.1 Processing Steps

In producing the enhanced resolution SSM/I and AMSR-E images, multiple passes are combined, using all the passes within a narrow time window at the same local time of day at each pixel. A detailed description of the local time-of-day image creation is contained in Gunn (2007). The averaging is split into morning and evening passes to remove artifacts introduced by diurnal brightness temperature variations during the day in summer. At low latitudes, there are essentially only two times of day approximately 12 hours apart for which brightness temperature

measurements can be obtained. At the poles, there is a spread, up to a few hours, in the local time-of-day of the observations. For SSM/I, by splitting the data by local time-of-day at 0800 and 2000 hours, the two data sets have narrow local time-of-day distributions, and thus similar brightness temperature values. The only complication to this scheme is that, as the local time-of-day is a function of longitude, there must be a longitude at which the day changes. This is normally at 180 degrees East.

In the North polar region, afternoon corresponds to the period 0500 through 1700 and night corresponds to 1700 through 2900, which is actually the next calendar day. Hence, the data are not all from the same calendar day. For the South pole, these times are altered to 0800 through 2000 and 2000 through 3200. These times are based on natural splits in the data. The images are originally produced in polar stereographic at the poles and Lambert Equal Area elsewhere. The images are then remapped to produce EASE-Grid north, south, and global views. Note: This method means that the EASE-Grid images do not show some portions of swaths over the ocean that were not included in the original land images.

3.3.2 Version History

Table 5 outlines the processing and algorithm history for this product.

Table 5. Version Details

Version	Date	Description
V01	Jul 2011	Original version of data.

3.3.3 Error Sources

While a local time-of-day processing was used to minimize variations in the surface (since the surface does not change much over a few hours), the atmosphere can change fairly rapidly. Thus, a change in brightness temperature distribution when combining all passes to produce this high resolution data set can produce image artifacts. While all images can have artifacts, they are most evident at 85 and 89 GHz due to atmospheric effects. Though the 85 and 89 GHz channels were chosen for their atmospheric sensitivity, it can be argued that multi-pass resolution enhancement for these channels may not be applicable for some studies.

A number of errors have been introduced in the SSM/I time series. However, with the exception of geolocation errors, SSM/I F13 data are largely devoid of such errors. Refer to the Error Sources section of the DMSP SSM/I-SSMIS Daily Polar Gridded Brightness Temperatures product for complete information regarding all error sources.

Level-2A AMSR-E used in the derivation of this data set include unsmoothed Level 1B data derived from antenna temperatures. Refer to the AMSR-E Instrument Description Web page for a description of the error sources associated with radiometer calibration. More information is also provided in the Error Sources section of the AMSR-E/Aqua L2A Global Swath Spatially-Resampled Brightness Temperatures user guide.

3.4 Sensor or Instrument Description

The instruments used to acquire these data are the SSM/I instrument on the Defense Meteorological Satellite Program (DMSP) F-13 satellite and the Advanced Microwave Scanning Radiometer - Earth Observing System (AMSR-E) instrument on the NASA Aqua satellite.

The SSM/I instrument is a seven-channel, four-frequency, orthogonally polarized, passive microwave radiometric system. The instrument measures combined atmosphere and surface radiances at 19.3 GHz, 22.2 GHz, 37.0 GHz and 85.5 GHz. Refer to the SMMR, SSM/I, and SSMIS Sensors Summary for more details.

The AMSR-E is a twelve-channel, six-frequency, conically-scanning, passive microwave radiometric system. It measures combined atmosphere and surface radiances ranging from 6.9 GHz to 89.0 GHz. Refer to the AMSR-E Instrument Description for more details.

4 REFERENCES AND RELATED PUBLICATIONS

Long, D. G., P. Hardin, and P. Whiting. 1993. Resolution Enhancement of Spaceborne Scatterometer Data. *IEEE Trans. Geosci. Remote Sens*. 31: 700-715.

Long, D. G. and D. Daum. 1998. Spatial Resolution Enhancement of SSM/I Data. *IEEE Trans. Geosci. Rem. Sens.* 36: 407-417.

Long, D. G., D. Early, and M. R. Drinkwater. 1994. Enhanced Resolution ERS-1 Scatterometer Imaging of Southern Hemisphere Polar Ice. Proc. Int. Geosci. Rem. Sens. Sym., Pasadena, California, 8-12 August, 156-158.

Long, D. G. and M. R. Drinkwater. 1999. Cryosphere Applications of NSCAT Data. *IEEE Trans. Geosci. Remote Sens*. 37 (3): 1671-1684.

Early, D. S. and D. G. Long. 2001. Image Reconstruction and Enhanced Resolution Imaging from Irregular Samples. *IEEE Trans. Geosci. Remote Sens.* 39 (2): 291-302.

Gunn, B. 2007. Temporal Resolution Enhancement for AMSR Images. MERS Technical Report 07-02, 04 Dec. 2007. http://www.scp.byu.edu/docs/pdf/MERS0702.pdf

Hollinger, J. P. and R. C. Lo. 1983. *SSM/I Project Summary Report.* Naval Research Laboratory. NRL Memorandum Report 5055. 106 pp.

Stroeve, J. 1998. Impact of Various Processing Options on SSM/I-Derived Brightness Temperatures. NSIDC Special Report-7.

5 CONTACTS AND ACKNOWLEDGMENTS

David Long
Microwave Earth Remote Sensing (MERS) Laboratory
Brigham Young University (BYU)
459 Clyde Building
Provo, Utah 84602 USA

Julienne Stroeve
National Snow and Ice Data Center (NSIDC)
Cooperative Institute for Research in Environmental Sciences (CIRES)
449 UCB, University of Colorado at Boulder
Boulder, Colorado 80309-0449 USA

Acknowledgments:

This research was supported by National Aeronautics and Space Administration (NASA) grant #NNG04GG72A.

6 DOCUMENT INFORMATION

6.1 Publication Date

July 2011

6.2 Date Last Updated

16 February 2021